GERARD BEGNI
Centre National d'Etudes Spatiales
31055 Toulouse Cedex, France

Selection of the Optimum Spectral Bands for the SPOT Satellite

The spectral bands were optimized by taking into account both the spectral signature of ground objects and the modifications introduced by the atmosphere.

THE SPOT SYSTEM

REMOTE SENSING OBSERVATIONS OF SPECTRAL SIGNATURES

CONSIDER AN OBJECT on the ground having a certain reflectance (Lambertian or not) $\rho(\lambda)$, where λ is wavelength. In the absence of the atmosphere, the radiance L_λ of this object in the direction of observation will, by definition, be given by

$$L_\lambda = \frac{E_{s_\lambda} \rho(\lambda) \cos \Theta_s}{\pi}$$

Observation systems provide a spectral analysis in a certain number of bands, and the spectral sensitivities of these bands vary with wavelength. We describe these sensitivities as $S_k(\lambda)$, where k is the characteristic index of a particular band. The quantity measured is of the form

$$x_k = A_k \int_0^\infty S_k(\lambda) \hat{L}_\lambda \, d\lambda$$

To characterize the above integral in a physical way as a unique number, we use $S_k(\lambda)$ as a normalizing function. The simplest way to do this is to use conventional formula of averages, and write

ABSTRACT: *The SPOT/HRV system provides images in three spectral bands of wave-length intervals 0.5 to 0.59 μm, 0.61 to 0.68 μm, and 0.79 to 0.89 μm, all at resolutions of 20 m, and in a panchromatic band from 0.51 to 0.73 μm with a resolution of 10 m. The system provides the facility for looking in the nadir direction or at a pointing angle of out to 27°, which is one of its major innovations. This paper deals with the choice of the locations and widths of the panchromatic and multispectral bands.*

We optimized the spectral bands for SPOT by taking into account both the spectral signature of ground objects and the modifications introduced by the atmosphere. In particular, we separated the spectral band B3 response from the absorption bands of water vapor and reduced the width of the panchromatic band, which was initially 0.50 to 0.90 μm.

We show how the system characteristics influence the measurement of spectral signatures formed by the three optimized bands. Signal-to-noise ratio, transfer function, and the problem of relative calibration were considered, but we report here only the results of a study of the influence of the atmosphere. We also show how the panchromatic band width was chosen by studying the contrast over thematically characterized objects.

where E_{s_λ} is the solar irradiance and Θ_s is the angle between the sun's direction and the surface normal. The atmosphere modifies this radiance as described later; the satellite then sees a modified radiance $\hat{L}_\lambda$, to which we can associate an apparent refectance $\hat{\rho}(\lambda)$ defined by

$$\hat{\rho}(\lambda) = \frac{\pi \hat{L}_\lambda}{E_{s_\lambda} \cos \Theta_s}$$

$$\hat{L}_k = \frac{\int_0^\infty S_k(\lambda) \hat{L}_\lambda \, d\lambda}{\int_0^\infty S_k(\lambda) \, d\lambda}$$

where $\hat{L}_k$ is a quantity equivalent to spectral radiance; it represents the weighted average of $\hat{L}_\lambda$ in the band. Note that if $\hat{L}_\lambda$ equals L_o (a radiance independent of λ), then $\hat{L}_k = L_o$. We can express this by saying L_k is the spectral radiance of an ob-

PHOTOGRAMMETRIC ENGINEERING AND REMOTE SENSING, 0099-1112/82/4810-1613$02.25/0

ject whose radiance does not change with λ, giving the same signal as the object being considered (and, therefore, indiscernible from it). In this paper, L_k will be called the "equivalent radiance." Similarly, we can define the "equivalent solar irradiance" by

$$E_k = \frac{\int_0^\infty E_{s_\lambda} S_k(\lambda)\, d\lambda}{\int_0^\infty S_k(\lambda)\, d\lambda}$$

and the "equivalent reflectance" by

$$\hat{\rho}_k = \frac{\pi \hat{L}_k}{E_k \cos \Theta_s}$$

We can easily show that

$$\hat{\rho}_k = \frac{\int_0^\infty E_{s_\lambda} S_k(\lambda)\, \hat{\rho}(\lambda)\, d\lambda}{\int_0^\infty E_{s_\lambda} S_k(\lambda)}$$

where $\hat{\rho}_k$ (which we call the "reflectance in band k") is, therefore, the average value of $\rho(\lambda)$ weighted by $E_{s\lambda}$ $S_k(\lambda)$.

The k numbers $\hat{\rho}_k$ constitute the spectral signature of the object as produced by the observation system under consideration. It provides a set of outputs:

$$x_k = B_k \hat{\rho}_k E_k \cos \Theta_s$$

where B_k is the absolute calibration of the system. E_k varies, however, in practice because of the variation of the Earth-sun distance. We therefore have

$$E_k = E_{ko}\, \mu\, (J)$$

where J is the date of observation. This variation is in the neighborhood of 2 percent, and is an accurately known quantity.

In remote sensing, we can consider several ways of using $\hat{\rho}_k$:

- Methods requiring a knowledge of $\hat{\rho}_k$. These imply a knowledge of B_k.
- Methods requiring only a knowledge of ratios of $\hat{\rho}_k$ (and therefore a knowledge of the ratios of B_k, which represent the interband calibration of the system).
- Methods that do not require a knowledge of $\hat{\rho}_k$, but that classify families of $\hat{\rho}_k$ having sufficient similarity (nonsupervised classification) or being sufficiently similar to the $\hat{\rho}_k$ of an object whose image is used as a reference (supervised classification). This implies uniquely that the quantity B_k must be constant over the area of the image being studied (calibration "within a band" or relative calibration).

REVIEW OF ATMOSPHERIC EFFECTS

We shall review the atmospheric modification of object radiance, giving a range of $\hat{L}_\lambda$ values (that can be referred to $\hat{\rho}_k$ values) different from L_λ (the polarization is also changed).

Atmospheric effects are due to two phenomena, absorption and scattering, that attenuate a light beam when it encounters atmospheric "particles" (gas molecules, aerosols). The radiance observed by a satellite sensor viewing a point on the Earth's surface comprises several components, as shown in Figure 1:

- The most important component of irradiance of the point of interest is that due to direct, partly attenuated solar flux.
- A second source of irradiance of the point of interest is due to atmospherically scattered flux that has not been reflected from the ground.
- A third source of irradiance is reflected flux, from points other than the point under consideration, that is redirected by atmospheric scattering to be incident on the point of interest.
- These three components of irradiance are reflected from the ground, and a part of this reflected flux is directed toward the sensor. It is further attenuated by scattering and absorption before reaching the sensor.
- The radiance at the sensor includes flux reflected from points on the ground, other than the point under consideration, that is redirected by atmospheric scattering into the sensor.
- "Intrinsic atmospheric reflectance" is the main component of so-called "atmospheric path radiance" and refers to the radiant flux that, after single (6) or multiple (6 bis) scattering (see Figure 1), reaches the sensor without encountering the ground.

These different components are sensitive to different parameters. Thus, the atmospheric scattering due to gaseous molecules decreases rapidly with wavelength (proportionally to λ^{-4}: Rayleigh scattering explaining the blue color of the sky); the decrease is less rapid for aerosols and the color is whiter). The absorption by certain molecules (O_3, H_2O) is important at certain wavelengths; it is related to the total quantity of gas contained in the atmosphere, which is quite variable. The most im-

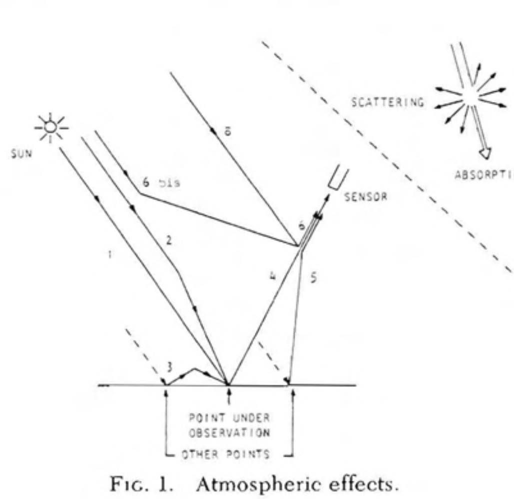

FIG. 1. Atmospheric effects.

portant parameters in the visible and the near infrared (0.45 to 1.1 μm) are

- The geometry: the angle Θ_s between the solar direction and the local normal, the angle Θ_v between the look direction and the surface normal, and the angle Θ_N between the solar and the look direction.
- The wavelength of interest.
- The concentration of aerosols, generally measured in terms of visibility (V = 23 km and V = 5 km are two cases typically studied).
- The ozone concentration (values fall between 0.25 and 0.45 cm atm.).
- The water vapor concentration (values generally range between 0.3 and 3 precipitable cm).

THE SPOT SYSTEM

We describe here only the system elements of direct interest within the scope of this paper, that is, the spectral bands and the geometric and radiometric resolutions. (Detailed information can be found in Chevrel *et al.* (1981) and Begni (1981).)

The SPOT system comprises two identical and independent instruments called HRV (high resolution visible). They provide three "spectral bands," the expected detailed profiles of which are given in Figure 2, normalized with respect to their maximum values. The bands are described by the wavelengths corresponding to the values at half the maximum values.

These are

B 1 : 0.50 – 0.59 μm
B 2 : 0.61 – 0.68 μm
B 3 : 0.79 – 0.89 μm

The "ground resolution" is 20 m. This means that the instrument, at any instant, measures the radiance spatially integrated over a given surface (this surface is the impulse response of the system, which is the convolution of optical diffraction, detector surface, smearing effect, and electronic interaction between detectors, and is roughly 20 by 30 m for the three spectral bands) and samples these data at 20-m intervals in two orthogonal directions. The HRV instruments also have a so-called "panchromatic band," the profile of which is also shown in Figure 2. The wavelengths corresponding to the values at half maximum are

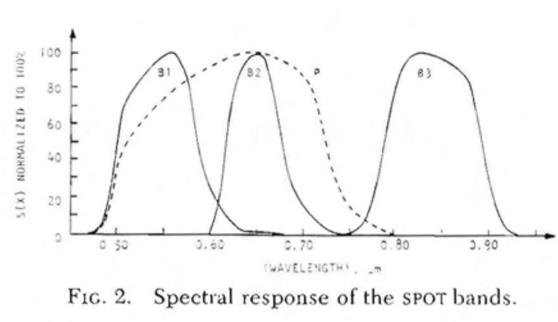

FIG. 2. Spectral response of the SPOT bands.

P : 0.51 – 0.73 μm

The ground resolution is 10 m.

Besides higher resolution, the major innovation of the SPOT system is the possibility of pointing the optical axis of the system perpendicularly to the velocity vector, out to an angle of 27°. The effective range corresponding to the ground look angle Θ_v is increased slightly due to the effect of Earth curvature. The major interest in "off-nadir viewing" is in applications such as repetitive coverage, rapid accessibility, and stereoscopy, but we can also foresee radiometric applications such as stereoradiometry.

The limitation of the "radiometric resolution" is related to noise, which introduces an uncertainty into the relationship between the incident value of $\hat{L}_\lambda$ and the output data (x_k). One must consider on the one hand the classical quantum and electronic noise contributions, and on the other hand the quantization noise, determined by the discrete nature of digitized data. The standard deviation of the distribution law describing this uncertainty is given by $Ne\Delta\hat{L}$. Consider two ground objects of reflectance ρ_A and ρ_B, independent of wavelength, in the band under consideration for a given atmospheric condition, the equivalent radiances outside the atmosphere being $\hat{L}_A$ and $\hat{L}_B$. If $\hat{L}_A - \hat{L}_B = Ne\Delta\hat{L}$, we can put $\rho_B - \rho_A = Ne\Delta\rho$, which corresponds to an effective variation on the ground equivalent to the instrumental noise, and depends on atmospheric conditions. The mission specification is $Ne\Delta\rho = 0.5 \times 10^{-2}$ for the output signal from the detector for $\Theta_v = 0$ and $15° < \Theta_s < 60°$, V = 23 km, $[O_3]$ = 0.35 cm, and $[H_2O]$ = 2 cm. In fact, when we consider an image as composed of the outputs from a large number of detectors (3,000 in the spectral bands and 6,000 in the panchromatic band), a residual relative calibration error exists that can be considered as a noise and has the effect of multiplying $Ne\Delta\rho$ by $(1 + \alpha)$, with $\alpha = 0.4$ for a zone of restricted dimensions and $\alpha = 0.7$ for an extended area (a SPOT scene measures 60 by 60 km).

The results of the studies that we present here concern vertical viewing only. Studies are in progress to evaluate the influence of the atmosphere on stereoradiometry.

STUDY OF SPECTRAL BANDS

DETAILED STUDY OF THE CHOICE AND PROFILES OF SPECTRAL BANDS

The choice of the three SPOT spectral bands was based on the most recently available spectral signatures of ground objects and on our ability to minimize the effect of the atmosphere upon them.

Most objects observed and readily studied by remote sensing techniques in the visible range do not show large changes in spectral reflectance within well defined regions. The exception is vegetation. A typical spectrum for vigorous vegetation shows a first local maximum at about 0.55 μm and a minimum at about 0.67 μm, followed by a rapid increase up to a plateau in the region of 0.75 μm (the amplitude of this plateau being much larger than that of the first maximum). It is possible to establish correlations between changes in vegetation and its spectral signature in these three spectral regions, which correspond to the three SPOT bands.

In fact, a detailed study can show that the two first bands are strongly correlated. So, for a first order purpose (such as vegetation discrimination), one may only use the two last spectral bands. However, because the second spectral band has a thematic meaning (absorption by chlorophyll), the subtle differences between spectral bands 1 and 2 may be used for thematic advanced studies such as vegetation disease.

A specific interest of the first spectral band is water penetration by its shorter wavelengths; this allows a detailed study of water in streams, lakes, and coastal zones.

The atmospheric perturbations must be taken into account, so as to minimize their influence on the measured spectral signatures.

The most important atmospheric effects are

- The rapid decrease of Rayleigh scattering ($1/\lambda^4$) as the wavelength increases, and the much less rapid change corresponding to scattering by aerosols.
- Absorption due to ozone; however, this is not a large transmission loss. The transmission is a minimum at about 0.60 μm and increases to a value of 1 at wavelengths of about 0.45 and 0.75 μm (see Table 1).
- The absorption due to water vapor; the transmission shows two local minima at about 0.72 and 0.81 μm and an important minimum at about 0.93 μm (see Table 1).

TABLE 1. ATMOSPHERIC TRANSMISSION OF OZONE AND WATER VAPOR

	Transmission of—	
Wavelength, μm	O_3	H_2O
0.45	0.99	1.00
0.46	0.99	1.00
0.47	0.99	1.00
0.48	0.99	1.00
0.49	0.88	1.00
0.50	0.97	1.00
0.51	0.97	1.00
0.52	0.96	1.00
0.53	0.95	1.00
0.54	0.94	1.00
0.55	0.94	1.00
0.56	0.92	1.00
0.57	0.91	1.00
0.58	0.91	1.00
0.59	0.91	1.00
0.60	0.90	1.00
0.61	0.91	1.00
0.62	0.92	1.00
0.63	0.93	1.00
0.64	0.94	1.00
0.65	0.95	1.00
0.66	0.96	1.00
0.67	0.97	1.00
0.68	0.98	1.00
0.69	0.98	0.99
0.70	0.98	0.98
0.71	0.99	0.91
0.72	0.99	0.85
0.73	0.99	0.94
0.74	0.99	0.99
0.75	0.99	1.00
0.76	0.99	1.00
0.77	1.00	1.00
0.78	1.00	0.99
0.79	1.00	0.99
0.80	1.00	0.98
0.81	1.00	0.82
0.82	1.00	0.86
0.83	1.00	0.90
0.84	1.00	0.99
0.85	1.00	1.00
0.86	1.00	1.00
0.87	1.00	1.00
0.88	1.00	0.99
0.89	1.00	0.83
0.90	1.00	0.83
0.91	1.00	0.78
0.92	1.00	0.75
0.93	1.00	0.22
0.94	1.00	0.28
0.95	1.00	0.29

$\Theta_s \simeq 41°$, $\Theta_v = 0$, $V = 23$ km, $[O_3] = 0.35$ cm atm., $[H_2O] = 2$ cm precip.

We also note that solar irradiance, which has a maximum at about 0.48 μm, decreases at longer wavelengths, so the irradiance at 0.82 μm is only about half that at 0.48 μm.

As a consequence of these considerations we see that

- In band B1, it is not possible to eliminate the influence of ozone absorption, however, we are interested in lowering, as much as possible, the response to short wavelengths in order to minimize the influence of Rayleigh scattering. In particular, we should center the band at the point of maximum sensitivity, which is at 0.55 μm, corresponding to the local maximum for vegetation.
- In band B2, it is also not possible to eliminate the influence of ozone absorption (which is weaker than in B1). In this case, we are measuring reflectance in a low reflectance region between two regions where it is high, so it is essential to block the band efficiently, in other words, to reduce, to the maximum extent possible, the residual transmission below 0.55 μm and above 0.69 μm. The former is easy but the latter is more difficult, for technological reasons, which is aggravating because of the high reflectance of vegetation as we approach the near infrared; thus, a residual very weak transmittance can produce a significant increase in the signal. A relative error of 10

TABLE 2. VALUES OF ρ_1^*, ρ_2^*, AND ρ_3^* (CORRESPONDING TO BANDS B1, B2, AND B3) FOR THE "IDEAL" AND "NOMINAL" CASES

ρ	"Ideal"			"Nominal"		
0.2	0.222,	0.207,	0.203	0.224,	0.212,	0.206
0.4	0.411,	0.403,	0.401	0.392,	0.392,	0.387
0.6	0.606,	0.601,	0.601	0.570,	0.579,	0.574
0.8	0.808,	0.802,	0.801	0.757,	0.771,	0.764

percent in the measurement of the reflectance of vegetation in this band can result.

In band B3 it is possible to reduce the influence of water vapor absorption by limiting the response of the band to wavelengths less than 0.89 μm. This cutoff is not sharp, again for technological reasons, but the residual effects are minimized by restricting the wavelength range in this manner.

GROUND REFLECTANCE AND REFLECTANCES OUTSIDE THE ATMOSPHERE IN THE THREE SPOT BANDS

In this section we shall determine the spectral signature in the three SPOT bands of an object of assumed known ground reflectance (which is also for convenience constant). We shall consider a set of standard conditions for SPOT corresponding to an equinox at 45°N latitude and with a nadir look angle. The atmospheric parameters for the "nominal case" are V = 23 km, $[H_2O]$ = 2 cm precipitable, and $[O_3]$ = 0.35 cm atmos. We shall vary each of these parameters and study the cases for ρ = 0.2, 0.4, 0.6, and 0.8 over a large surface. We shall determine the three values $\hat{\rho}_1$, $\hat{\rho}_2$, and $\hat{\rho}_3$ for each case. The study has been performed with models developed by the "Laboratoire d'Optique Atmosphérique" in Lille, France (Deschamps *et al.*, 1981).

"Ideal" and "Nominal" Cases. First we present the results for an unrealizable "ideal" case, where there are no aerosols, ozone, or water vapor, and for the "nominal" case. These are shown in Table 2.

In the "ideal" case, $\hat{\rho}$ is always greater than ρ; this is because of the high transmittance of the atmosphere and the reflectance of the atmosphere itself. The latter effect decreases with wavelength; it is almost negligible in bands B2 and B3. For high reflectances, absorption and scattering compensate each other, which makes the differences between ρ and $\hat{\rho}$ small.

In the "nominal" case the phenomena are more complex. We have $\hat{\rho} > \rho$ for low reflectances, but the decrease with wavelength is less marked than for the "ideal" case. For average and high reflectances, absorption decreases the apparent reflectance; ozone has certain observable effects on $\hat{\rho}_1$ and $\hat{\rho}_2$; so does water vapor for $\hat{\rho}_3$ (see, in particular, the case for ρ = 0.8).

Visibility. Table 3 shows the changes in reflectance with visibility, everything else being held constant. ("nominal case" values)

The reflectance of the atmosphere itself increases with the presence of aerosols. This is why for low reflectances we observe an increase of $\hat{\rho}$ with decreasing visibility, corresponding to increasing aerosol concentration. The influence of atmospheric scattering is not negligible in band B3, because aerosol scattering is much less wavelength dependent than Rayleigh scattering. We have $\hat{\rho} > \rho$ for ρ = 0.2 except in the Rayleigh case for bands B2 and B3 (absorption due to water vapor and ozone). For average and high reflectances the absorption due to aerosol, water, and ozone makes $\hat{\rho} < \rho$. The change with wavelength is variable (in particular, compare ρ = 0.8, V = 5 km; ρ = 0.8, V = 23 km; and ρ = 0.4, V = 23 km). For average reflectances the tendency is for $\hat{\rho}$ to increase with incresing aerosol concentration; for high reflectances, the tendency is for it to decrease.

Ozone Concentration. Table 4 shows the change in $\hat{\rho}$ with ozone concentration, everything else being held constant ("nominal" case values).

This table confirms that ozone has no influence in band B3. The case of $[O_3]$ = 0 is an artificial case, and is given only for reference. Ozone causes absorption only; so it is observed that $\hat{\rho}$ decreases when the ozone concentration increases. For low reflectances, $\hat{\rho}$ is always greater than ρ because of the reflectance of the atmosphere itself, but this situation is reversed for ρ = 0.4 for realistic concentrations of ozone. Note that the effect is more pronounced for band B1 than for B2; for ρ = 0.8, the loss from 0.25 cm atm. to 0.45 cm atm. is $\Delta\hat{\rho}$ = 0.03 for B1 and 0.01 for B2.

Water Vapor Concentration. Table 5 shows the change in $\hat{\rho}$ with water vapor concentration.

TABLE 3. VALUES OF $\hat{\rho}_1$, $\hat{\rho}_2$, AND $\hat{\rho}_3$ FOR DIFFERENT CONCENTRATIONS OF AEROSOLS (EXPRESSED AS VISIBILITIES)

	Visibility V								
ρ	Rayleigh			23 km			5 km		
0.2	0.208,	0.196,	0.191	0.224,	0.212,	0.206	0.258,	0.245,	0.237
0.4	0.384,	0.381,	0.377	0.392,	0.392,	0.387	0.405,	0.409,	0.405
0.6	0.566,	0.569,	0.564	0.570,	0.579,	0.574	0.561,	0.582,	0.581
0.8	0.755,	0.759,	0.752	0.757,	0.771,	0.764	0.728,	0.766,	0.767

TABLE 4. VALUES OF $\hat{\rho}_1$, $\hat{\rho}_2$, AND $\hat{\rho}_3$ FOR DIFFERENT OZONE CONCENTRATIONS

	$[O_3]$, cm atmos.											
ρ	0			0.25			0.35			0.45		
0.2	0.239,	0.216,	0.206	0.228,	0.213,	0.206	0.224,	0.212,	0.206	0.220,	0.211,	0.206
0.4	0.419,	0.399,	0.387	0.400,	0.394,	0.387	0.392,	0.392,	0.387	0.385,	0.390	0.387
0.6	0.609,	0.589,	0.574	0.581,	0.581,	0.574	0.570,	0.579,	0.574	0.559,	0.576,	0.374
0.8	0.809,	0.785,	0.764	0.771,	0.775,	0.764	0.757,	0.771,	0.764	0.743,	0.767,	0.764

The table shows that water vapor has no effect on band B1. (As for ozone, the case for $[H_2O] = 0$ is an artificial case, included only for reference.) Again, we note that $\hat{\rho}$ decreases with increase in water vapor concentration; the effect is more pronounced for band B3 than for band B2.

For $\rho = 0.8$, the loss between water vapor concentrations of 0.5 cm and 5 cm is $\Delta\hat{\rho} = 0.03$ in band B2 and 0.05 in band B3.

Conclusions. In conclusion we see that $\hat{\rho}_1$, $\hat{\rho}_2$, $\hat{\rho}_3$ are not grossly different from ρ_1, ρ_2, ρ_3 but that the differences are, nevertheless, significant. It is important to note that variations in $\hat{\rho}_1$, $\hat{\rho}_2$, $\hat{\rho}_3$ are a function of atmospheric parameters. Variations on the order of $\Delta\hat{\rho} = 0.05$ are possible between two extreme values of the parameters. These extreme values are realistic on a world-wide basis.

However, for a given region it is always worthwhile to determine in detail the range of atmospheric parameter changes that can be anticipated, noting that the range will probably be smaller than that studied here.

CONSIDERATION OF THE PANCHROMATIC BAND

The width of the panchromatic band makes it of little interest for spectral signature studies because spectral changes in ground features are averaged out across its width. Its value lies more in photointerpretation, cartography, etc. This is, of course, a generality and is not always true.

The study of spectral reflectances provides us a way to determine how the integration over a wide band can enhance or reduce the contrast between objects having different characteristics. Two kinds of panchromatic bands are commonly used: 0.5 to 0.7 μm (visible) and 0.5 to 0.9 μm (visible and near IR). The latter is used for meteorological satellites because it provides good discrimination among water, damp soil, and vegetation. This is valuable for satellites having resolutions of several kilometres.

A satellite system having a resolution of 10 m poses a different problem. Instrumental considerations (optimization of signal level), improvement of the transfer function and, therefore, the effective resolution) tend to impose the former solution; however, thematic considerations may modify that solution.

We considered the problem as follows:

We selected a certain number of spectral distributions $\rho(\lambda)$ corresponding to gray granite, red clay, damp soil, vigorous sugar beet (strong IR reflectance), fallow ground, trees, and grass (moderate IR reflectance). We assumed the radiance outside the atmosphere, L_λ, to be given by the model described above. Then we chose a realistic model for the spectral sensitivity $S(\lambda)$ as a function of two parameters, λ_1, λ_2, in such a way as to simulate a panchromatic band, λ_1 to λ_2. We then determined the calibrated response of the instrument to several different targets as a function of λ_1 and λ_2 (for an instrument with a specific calibration, a reference distribution ρ (λ) gives a specific output). Figure 3 provides a graphical interpretation of the results: First, by varying λ_2 with λ_1 fixed at 0.5 μm and then varying λ_1 with λ_2 at 0.9 μm, we studied the response as a function of different cutoff wavelengths. The effect of varying λ_1 was inconsequential; it simply reduced the output signal from the instrument and was therefore not considered further. We proceeded to examine the effect on the response of the system of a change in λ_2.

If we consider vigorous vegetation, we see there is a more or less rapid increase in the signal when

TABLE 5. VALUES OF $\hat{\rho}_1$, $\hat{\rho}_2$, AND $\hat{\rho}_3$ FOR DIFFERENT WATER VAPOR CONCENTRATIONS

	$[H_2O]$, cm precipitable											
ρ	0			0.5			2			5		
0.2	0.224,	0.219,	0.218	0.224,	0.215,	0.212	0.224,	0.212,	0.206	0.224,	0.208,	0.199
0.4	0.392,	0.406,	0.411	0.392,	0.399,	0.399	0.392,	0.392,	0.387	0.392,	0.384,	0.375
0.6	0.570,	0.600,	0.610	0.570,	0.589,	0.592	0.570,	0.579,	0.574	0.570,	0.566,	0.554
0.8	0.757,	0.799,	0.813	0.757,	0.784,	0.788	0.757,	0.771,	0.764	0.757,	0.754,	0.738

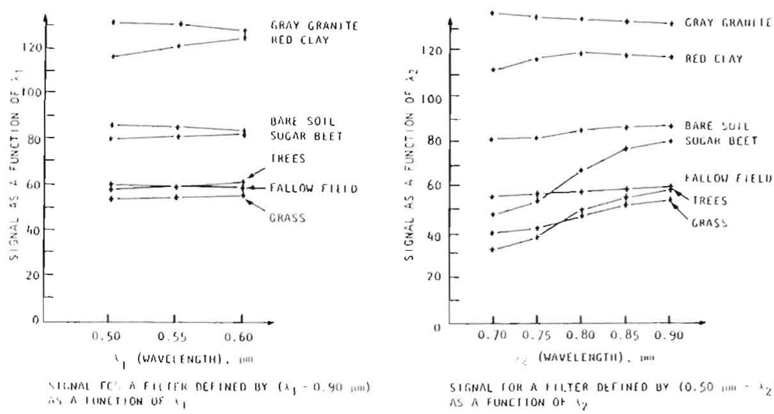

FIG. 3. Response of the panchromatic band to various test targets as a function of the cutoff wavelength.

λ_2 changes from 0.7 μm to 0.9 μm. For sugar beet this corresponds to an increase in signal by a factor of 1.7, and for trees by a factor of about 1.8. This is because of the rapid increase in reflectance of this type of feature at about 0.7 μm (considered earlier in detail with reference to band B2). These increases are partially offset by the decrease of solar irradiance, the absorption of water vapor, and the artificial increase of the signal in the blue due to Rayleigh scattering. On the other hand, vegetation that is not in vigorous growth, rocks, and targets consisting of asphalt or concrete don't vary much.

We can distinguish two tendencies:

- The choice of a band between 0.5 and 0.9 μm provides contrast between different types of vegetation, which is related to the degree of vigor of vegetation. However, the increase of the signal of crops like sugar beet approaches that of bare soil, and there is therefore the possibility of confusion between the two different signatures. The choice of a band between 0.5 and 0.9 μm can help identify a class but also creates the risk of confusing it with another. The possibility of confusion is very real because, in our opinion, the curves presented for rock are too high (laboratory samples) and, therefore, the derived numerical values should be smaller. This would increase the confusion between the two classes. Certain types of rock (schists) have low reflectance and are often confused with vegetation; the same applies to asphalt, but experience shows that roads are easily recognized because of their context (long straight lines crossing varied thematic areas).
- The use of a band from 0.5 to 0.7 μm reduces the signal due to vegetation. It makes the contrast between different types of vegetation less perceptible (this contrast can be studied in the third spectral band because the 10 metres resolution is not critical) but on the other hand improves the differentiation between vegetation and bare soils, rocks, or artefacts.

We have not evaluated the situation for water. Calm, pure water (not close to the condition of specular reflection) shows very low reflectance, decreasing with wavelength, and is very easily distinguished on panchromatic images.

A more difficult situation is damp soil, for which the reflectance is between that of dry soil and of water; it is lower than that for dry soil, decreasing with wavelength. There is, therefore, a tendency to confuse damp soil with vegetation, and this is more noticeable for a band from 0.5 to 0.9 μm than one from 0.5 to 0.7 μm because of the increase in the signal provided by vegetation and the slow drop in signal due to soil. Therefore: (1) For satellites with low resolution (SMS, Meteosat), it is desirable to have a high contrast between dry and damp regions on a scale compatible with the resolution of the satellite; we prefer the band between 0.5 and 0.9 μm, which accentuates contrast, the distinction between vegetation and damp soil being less important. We can say, a posteriori, that the panchromatic Meteosat (0.5 to 0.9 μm) is of more value than the panchromatic SMS (0.5 to 0.7 μm) for this goal. (2) For a satellite with high resolution, the contrast between dry and damp regions is at far too large a scale, and we want to be able to observe much finer detail. We have, therefore, chosen a band from 0.5 to 0.7 μm, which reduces the confusion caused by moisture on the contrast between bare soil and vegetation. (This band is the usual IGN (Institut Géographique National) choice for photography in the panchromatic mode.)

Because the transfer function of CCDs is better for shorter wavelengths, this choice tends to improve the geometric resolution, as we previously said.

As a final point, Figure 3 shows that the limit λ_2 = 0.7 μm can be moved to 0.73 μm; this is desirable to increase the signal-to-noise ratio of the system. The panchromatic passband chosen is shown in Figure 2.

This theoretical study has been validated thanks to SPOT simulations. An airborne scanner (DAEDALUS) has been used to collect multispectral images of selected areas. Different panchromatic bands can be synthetized by linear weighted combinations of the original channels (see Saint *et al.* (1981) for details). The two kinds of panchromatic bands can easily be separated; the transition can be observed for $\lambda = 0.75\ \mu m$ approximately.

ACKNOWLEDGEMENT

Most of the thematic information used in this study was provided by M. Saint, CNES Toulouse. The atmospheric model was developed by M. Deschamps, Laboratoire d'Optique Atmospherique, Lille.

Prof. P. N. Slater, University of Arizona, Committee on Remote Sensing, has reviewed a preliminary version of this paper.

REFERENCES

Begni, G., 1981. Image Quality for SPOT satellite: specifications and budget. IAF 1981—XXXII Congress—C.2 Symposium.

Chevrel, M., M. Courtois, and G. Weill, 1981. The SPOT satellite Remote Sensing Mission, *Photogrammetric Engineering and Remote Sensing*, Vol. 47, No. 8, August 1981, pp. 1163-1171.

Deschamps, P. Y., M. Herman, and D. Tanre, 1981. Atmospheric influence in earth resources remote sensing (visible and infrared) modelization and correction possibility, *Proceedings of the International colloquium ISP Avignon* (France), September 1981, "Spectral Signatures of objects in remote sensing," pp. 543-558.

Saint, G., A. Podaire, and I. Anglade, 1981. SPOT Radiometric simulations; results of experiments on vegetation and soils. *Proceedings of the International colloquium ISP Avignon* (France), September 1981, "Spectral Signatures of objects in remote sensing," pp. 73-83.

Tucker, C. J., 1978. A comparison of satellite sensor bands for vegetation monitoring *Photogrammetric Engineering and Remote Sensing*, Vol. 44, pp. 1369-1380.

(Received 5 March 1982; accepted 25 April 1982)

CALL FOR PAPERS

Seventeenth International Symposium on Remote Sensing of Environment

Ann Arbor, Michigan
9-13 May 1983

Sponsored by the Environmental Research Institute of Michigan (ERIM), the Symposium will address state-of-the-art capabilities and techniques, as well as new or innovative concepts in scientific research and development, leading to a better understanding of the technology and its effective application. Conventional sessions and multidisciplinary poster sessions will be formulated to address

- New or innovative techniques and methodology
- Advanced sensor and data acquisition system design
- Advanced data processing and analysis capabilities
- Earth resources, environmental monitoring, and information system requirements
- Discipline or mission oriented projects leading to operational utilization of the technology.

All persons interested in contributing a paper for consideration for poster presentation should submit a 300 to 1000 word summary providing a brief justification for the work, program, or concept reported, and an explanation of its relation to the current state-of-the-art or to development of the specific application involved. Additionally, each summary submitted should provide details of any results obtained to date; and, in the case of a new or innovative approach, should provide a brief discussion of how the concept, technique, or methodology differs from existing methods.

Twenty copies of the summary, in English, should be submitted by *1 November 1982* to

Dr. Jerald J. Cook
Environmental Research Institute of Michigan
P.O. Box 8618
Ann Arbor, MI 48107
Tele. (313) 994-1200